FDTD Characterization of Evanescent Modes—Multimode Analysis of Waveguide Discontinuities

Enrique A. Navarro, *Member, IEEE,* Thamar M. Bordallo, and Joaquín Navasquillo-Miralles

***Abstract*—In this paper, a finite-difference time-domain numerical dispersion relation for evanescent waves is derived, and its impact on the modeling accuracy is studied. The numerical evanescent constant is found to differ from the analytical one. As a result, a correction must be used to compute discontinuity parameters. This influences the reference plane chosen for the analysis of propagating modes. Moreover, on calculating multimode transmission and reflection coefficients, the dispersion for evanescent higher order modes is determinant. The dispersive relation is derived, discussed, and used to correct the evanescent constants for the multimode analysis of a waveguide discontinuity.**

***Index Terms*—Evanescent modes, FDTD methods, numerical analysis, scattering matrices, waveguide discontinuities.**

I. Introduction

THE finite-difference time-domain (FDTD) method is a well-established tool for the microwave engineering community. Thus far, the FDTD method has been applied to model microwave circuits and antennas [1]. The usual procedure to analyze a given device, using FDTD, involves the following steps:

- *Step 1:* use of a fine mesh to avoid numerical dispersion, suitable to establish boundary conditions;
- *Step 2:* application of an effective absorbing boundary condition (ABC);
- *Step 3:* selection of a suitable excitation in space and time;
- *Step 4:* verification of FDTD results by comparison with other techniques or measurements.

If FDTD results present a good agreement in Step 4, Steps 1–3 will be extended to the next device sharing similar geometry. If not, Steps 1-3 must be revised. Once Step 4 has been achieved successfully, simulated results in subsequent applications of FDTD are expected to be as accurate as in the first application. The procedure is considered to be consistent and warranties a bound in the FDTD results. Some studies have addressed the accuracy of the FDTD modeling [2], with the conclusion that second-order accuracy is achieved with the FDTD discretization. However, this second-order accuracy can be polluted by inaccurate ABC's, numerical dispersion [2]–[4], and inaccurate post-processing of the FDTD simulated data. An example can be found in the application of the fast Fourier transform (FFT): the freedom of the user to locate a window in the FDTD-space time to which the FFT is applied may result in different accuracy of the FDTD results.

In the analysis of waveguide discontinuities, a typical situation is produced when choosing the points at which the transmitted fields are sampled. At these points, evanescent higher order modes are expected to be negligible, in order to get a clean dominant propagating mode at the outputs of the FDTD simulated device. An FDTD user must be cautious in choosing the sampling planes; the further the better, but with larger memory resources because longer waveguide ports must be meshed. This increases the consumption of memory and central processing unit (CPU) time [5]. The optimum length of a waveguide port is the shortest that warranties negligible higher order evanescent modes while providing sufficient accuracy for the dominant mode. Determining the optimum length can be done by a systematical error analysis in FDTD, as will be shown in this paper. In the numerical domain of FDTD, evanescent modes are found to decay more slowly than the analytically calculated modes. The numerical evanescent constant is different from the analytically obtained one. Consequently, knowledge of a numerical evanescent constant can be used to estimate the waveguide ports length. In particular, in the calculation of multimode scattering parameters of a waveguide discontinuity, an appropriate reference plane needs to be located by using the numerically calculated evanescent phase constant. Large errors are produced in the calculation of the multimode parameters unless the proper evanescent constant is used.

Thus far, the FDTD technique has been successfully used in the analysis of waveguide discontinuities where the scattering parameters were obtained for the fundamental TE_{10} propagating mode. ABC's warranted the accuracy of the simulation for the propagating modes. In [6], the multimode transmission coefficients were calculated for a two-dimensional discontinuity in which second-order absorbing boundaries were used to absorb evanescent waves. In the analysis, numerical dispersion was neglected and results were obtained for two propagating modes and two evanescent modes for a given frequency [7]. In [8], FDTD is combined with modal expansion.

In our calculation of multimode parameters, the numerically calculated evanescent constants are used to shift the parameters to the reference plane. In this study, perfectly matched layers (PML's) are used [9]–[11], to absorb any mode at any frequency, where it does not matter whether the mode is evanescent or not

Manuscript received July 2, 1998. This work was supported by the Universitat de Valencia under Project UV98-2719, and by the Generalitat Valenciana under Project GV98-14-126.

The authors are with the Department of Applied Physics, Universitat de València, 46100 Burjassot, València, Spain.

Publisher Item Identifier S 0018-9480(00)02779-4.

[12], [13]. The application of PML's in a small three-dimensional mesh enables one to obtain the general scattering matrix (GSM) of any step discontinuity. To show the utility and accuracy of our procedure, results are presented for a transition between two waveguides of different dimensions.

Once the multimode parameters are obtained, the application of the GSM formalism can provide the electrical modeling of any complex device by cascading the multimode parameters that are obtained with FDTD for each simple discontinuity.

II. Dispersion Relation

Assume a plane wave in the discretized three-dimensional FDTD space with the wave being a propagating wave or an evanescent wave. A propagating plane wave would have the space-time dependence $\vec{E}(x,y,z,t) = \vec{E}_0(t) \cdot e^{-j\vec{k}\vec{r}}$, $\vec{k}$ being the wave vector and $\vec{r}$ the position vector. By substituting it into the Maxwell equations and performing numerical derivatives, the following expression is obtained:

$$-4\left[\frac{\sin^2\left(\frac{k_x\Delta x}{2}\right)}{\Delta x^2}+\frac{\sin^2\left(\frac{k_y\Delta y}{2}\right)}{\Delta y^2}+\frac{\sin^2\left(\frac{k_z\Delta z}{2}\right)}{\Delta z^2}\right] = \mu\epsilon\frac{\lambda^2-2\lambda+1}{\lambda\Delta t^2} \quad (1)$$

where the standard notation $\vec{E}^n(i,j,k) = \vec{E}(i\Delta x, j\Delta y, k\Delta z, n\Delta t)$ was used, and $\lambda = (E_l^{n+1}/E_l^n)$, $(l \equiv x,y,z)$ is defined as the numerical growth factor [14]–[16]. The above equation is solved for λ, and the stability condition $|\lambda| \leq 1$ implies the following expression:

$$\sqrt{\frac{\sin^2\left(\frac{k_x\Delta x}{2}\right)}{\Delta x^2}+\frac{\sin^2\left(\frac{k_y\Delta y}{2}\right)}{\Delta y^2}+\frac{\sin^2\left(\frac{k_z\Delta z}{2}\right)}{\Delta z^2}}\Delta t \leq \sqrt{\mu\epsilon} \quad (2)$$

for any wave vector $\vec{k}$. This leads to the well-known FDTD stability condition

$$c\Delta t \leq \frac{1}{\sqrt{\frac{1}{\Delta x^2}+\frac{1}{\Delta y^2}+\frac{1}{\Delta z^2}}} \quad (3)$$

where $c = (1/\sqrt{\mu\epsilon})$.

Similarly, for a monochromatic plane wave, with time dependence in the form $e^{j\omega t}$, the substitution into the vector wave equation

$$\vec{\nabla}\times\vec{\nabla}\times\vec{E} - \mu\epsilon\frac{\partial^2\vec{E}}{\partial t^2} = 0 \quad (4)$$

leads to the well-known dispersion relation of FDTD

$$\frac{\sin^2\left(\frac{k_x\Delta x}{2}\right)}{\Delta x^2}+\frac{\sin^2\left(\frac{k_y\Delta y}{2}\right)}{\Delta y^2}+\frac{\sin^2\left(\frac{k_z\Delta z}{2}\right)}{\Delta z^2} = \mu\epsilon\frac{\sin^2\left(\frac{\omega\Delta t}{2}\right)}{\Delta t^2}. \quad (5)$$

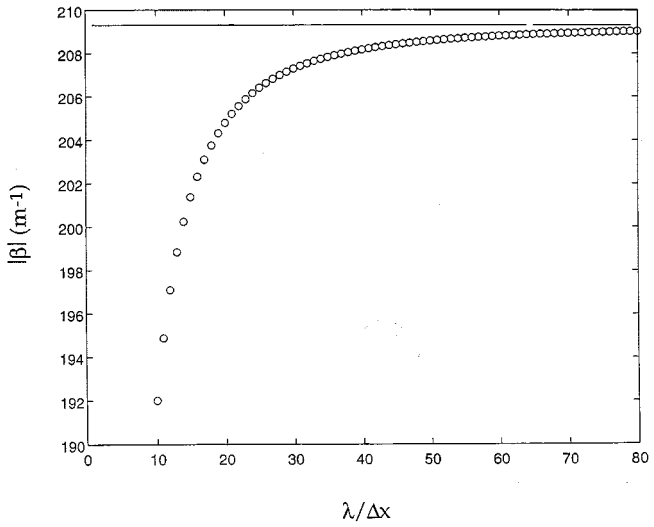

Fig. 1. Evanescent constant for TE_{20} mode under cutoff as a function of the FDTD discretization $\Delta x = \Delta y = \Delta z$.

Now, let us consider an evanescent plane wave decaying in the z-direction. Its analytical form can be expressed as $\vec{E}(x,y,z,t) = \vec{E}_0(t) \cdot e^{-j(k_x x + k_y y)} \cdot e^{-k_z z}$. By substitution of this electric field into the Maxwell' equations and performing the mathematical manipulations similar to those for the propagating wave, the following stability condition is obtained:

$$c\Delta t \leq \frac{1}{\sqrt{\frac{1}{\Delta x^2}+\frac{1}{\Delta y^2}-\frac{\sinh^2\left((k_z\Delta z/2)\right)}{\Delta z^2}}}. \quad (6)$$

The new dispersion relation for the evanescent wave then becomes

$$\frac{\sin^2\left(\frac{k_x\Delta x}{2}\right)}{\Delta x^2}+\frac{\sin^2\left(\frac{k_y\Delta y}{2}\right)}{\Delta y^2}-\frac{\sinh^2\left(\frac{k_z\Delta z}{2}\right)}{\Delta z^2} = \frac{\sin^2\left(\frac{\omega\Delta t}{2}\right)}{c^2\Delta t^2}. \quad (7)$$

The above numerical dispersion relation approaches the analytical dispersion relation $(\omega^2/c) = k_x^2 + k_y^2 - k_z^2$ only in the limit $\Delta x, \Delta y, \Delta z, \longrightarrow 0$.

Let us consider the particular case of a rectangular waveguide for the TE_{20} mode under cutoff. For a given frequency under cutoff, this would have an evanescent constant $\beta = \sqrt{(2\pi/a)^2 - \omega^2\mu\epsilon}$. Suppose that the waveguide has dimensions $a = 2.286$ cm, $b = a/2$, the TE_{20} mode cutoff frequency is then 13.12 GHz. If the given frequency is 8.5 GHz, the evanescent constant for the exponentially decaying field is 209.41 m^{-1}. However, the numerical value for this constant calculated from (7) is not the same. Its numerical FDTD dispersive value depends on the discretization. If $\Delta x = \Delta y = \Delta z$, and $\Delta t = 0.8\Delta x/c$, it starts from nearly zero value at $\Delta x = \lambda/3$ and moves toward the analytical value with the smaller space increment. These results are shown in Fig. 1 where it is seen that even for $\Delta x = \lambda/20$,

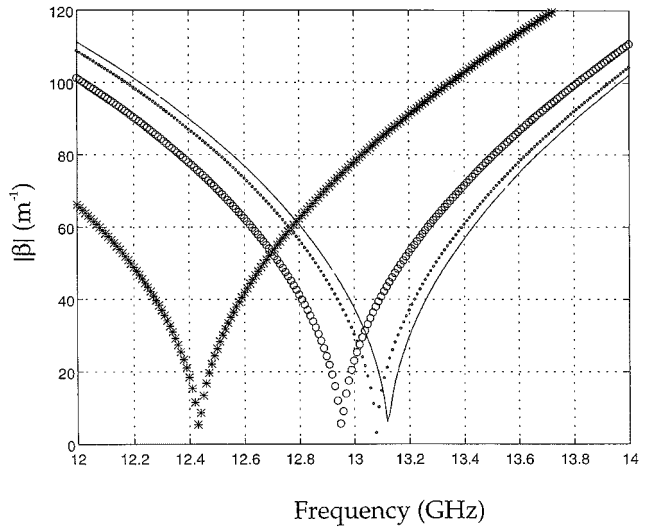

Fig. 2. Numerical FDTD and analytical dispersion relation ($|\beta|$ versus frequency), for TE_{20} mode using three different discretizations; $a = 2.286$ cm is the largest waveguide wall, $\Delta x = \Delta y = \Delta z$. (—): analytical. FDTD: $(*)\Delta x = a/5, (\mathrm{o})\Delta x = a/10, (\cdot)\Delta x = a/20$.

the numerical evanescent constant is only 206 m^{-1}, 3.1% lower than the analytical value. For the same TE_{20} mode, the numerical FDTD evanescent constant versus frequency is also calculated. The results of this investigation are presented in Fig. 2, where numerical and analytical dispersion relations were plotted versus frequency for three different discretizations ($\Delta x = a/5, \Delta x = a/10, \Delta x = a/20$). It shows that numerical cutoff frequency differs from the analytical value, and this difference increases with the coarseness of the mesh.

The influence of the above results is critical in the FDTD modeling of evanescent modes, especially in determining how far the FDTD sampling plane is away from the discontinuity or the region where these modes are generated. In the waveguide analysis for the dominant mode (TE_{10}), the influence of the numerical dispersion of evanescent modes can be avoided by placing the FDTD sampling plane far enough from any simulated discontinuity. The location of the plane is decided with the numerically calculated constants rather than the analytical ones as the numerical evanescent constants are smaller than the analytical ones. When FDTD simulation is carried out for higher order modes under cutoff, the numerical evanescent dispersion pollutes the behavior of the evanescent field, particularly when FDTD is used to calculate the multimode parameters of a given discontinuity. To avoid errors, the fields that are sampled close to the discontinuity must be corrected with the numerical evanescent constant.

III. FDTD Multimode Formulation

The transmitted and reflected fields in the waveguides at a short distance from the waveguide discontinuity can be expanded as a sum over all possible modes inside the waveguides. This total electric field at the time instant $t = n\Delta t$ can be expressed as

$$\vec{E}(\vec{r},t) = \sum_i \left[\vec{e}_i^{\,\mathrm{TE}}(\vec{r}) \cdot V_i^{\mathrm{TE}}(t)\right] + \sum_j \left[\vec{e}_j^{\,\mathrm{TM}}(\vec{r}) \cdot V_j^{\mathrm{TM}}(t)\right] \tag{8}$$

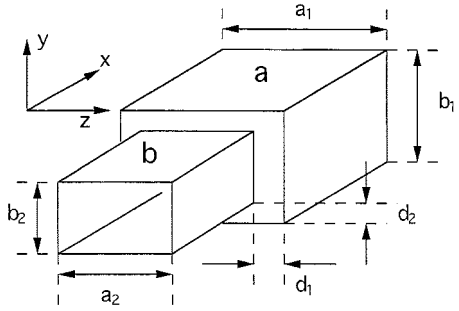

Fig. 3. Transition between two waveguides having different cross section. Waveguide a, $a_1 = 22.86$ mm, $b_1 = 12.70$ mm. Waveguide b, $a_2 = 19.05$ mm, $b_2 = 9.525$ mm, $d_1 = 1.905$ mm, $d_2 = 1.5875$ mm.

where $\vec{e}_i^{\,\mathrm{TE}}(\vec{r})$, and $\vec{e}_j^{\,\mathrm{TM}}(\vec{r})$ are the normalized mode vectors, and $V_i^{\mathrm{TE}}(t)$ and $V_j^{\mathrm{TM}}(t)$ are the mode voltages. Due to the orthogonality of the mode vectors, we can determine the mode voltages at any cross section by multiplying both sides of (8) with the corresponding mode vector and integrating over the waveguide cross section. Noting that the mode vectors are normalized, we obtain

$$\int_S \vec{E}(\vec{r},t) \cdot \vec{e}_i(\vec{r}) \cdot \, dS = V_i(t) \tag{9}$$

where i is the mode index for both TE and TM, in both sides of the discontinuity. The above integral is performed over the cross section S of the waveguide, and $\vec{E}(\vec{r},t)$ is the numerically simulated FDTD field at the cross section of the waveguide. The FFT of $V_i(t)$ gives $V_i(\omega)$. These coefficients are normalized and operated to give the multimode scattering parameters

$$S_{i,j}(\omega) = \frac{V_j(\omega) \cdot \sqrt{Z_i}(\omega)}{V_i(\omega) \cdot \sqrt{Z}_j(\omega)} \tag{10}$$

where $Z_i(\omega)$ is the impedance for mode i at the frequency ω. These parameters can be shifted to a phase reference plane by multiplying with the phase term $e^{j\beta_i \Delta l_i}$, and $e^{j\beta_j \Delta l_j}$ [17], l_i, l_j being the distances from the sampling planes to the reference planes; β_i, β_j are the propagating constants of the modes i and j, respectively. These propagation constants will be the evanescent constants under cutoff (evanescent higher order modes), i.e., $e^{-|\beta_i|\Delta l_i}$ or $e^{-|\beta_j|\Delta l_j}$.

In the following section, this procedure is used to calculate the multimode scattering parameters for a given sample discontinuity. In that calculation, the values of the evanescent propagation constants are corrected using the numerical dispersion relation obtained in Section II.

IV. Results

The above procedure is used to analyze a transition in waveguide that connects two rectangular waveguides with different dimensions. Waveguide a has the dimensions of 22.86 mm × 12.70 mm, and waveguide b has 19.05 mm × 9.525 mm, as shown in Fig. 3. The waveguide discontinuity was modeled using a 40 × 10 × 20 mesh in the x–y–z-directions, respectively. Twenty PML layers were used to simulate the matched loads at both sides of the discontinuity, with the conductivity having a profile $\sigma = \sigma_{\max} \cdot (l/l_{\max})^q$, where q and $\sigma_{\max}$ are

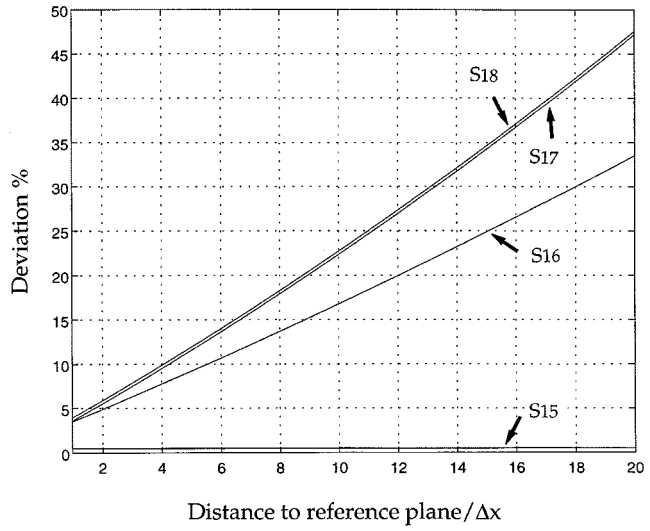

Fig. 4. Dependence of the deviation on the distance from the sampling plane to the reference plane. Results for $S_{1,j}$, $j = 5, 6, 7, 8$, frequency $= 9$ GHz.

adjusted for a theoretical reflection coefficient of -80 dB, [9], [12], [2]. $l_{\max}$ is the total thickness of the PML and l is the penetrating depth inside the PML region. The excitation consisted of a sinusoidally modulated pulse in the time domain whose spectrum covered the operating frequency band of the TE_{10} mode in the first waveguide (waveguide a in Fig. 3). The spatial distribution of the incident field was of the TE_{10} mode in the cross section of the waveguide a. The mode voltages of the transmitted and reflected signals were obtained for TE_{10}, TE_{30}, TE_{12}, TE_{32} modes in both waveguides. These modes are numbered 1-4 for waveguide a, and 5-8 for waveguide b. Therefore, the multimode reflection coefficients are $S_{1,j}$ for $j = 1, 2, 3, 4$ and the transmission coefficients are $S_{1,j}$, for $j = 5, 6, 7, 8$. Equation (9) is numerically integrated at every time step of the FDTD simulation over the cross section of both waveguides, five cells from the discontinuity. The reference plane chosen for the scattering parameters is the one where the discontinuity is located. The parameters shift [17] is done with the numerical evanescent constant obtained from (7). The used mode impedances are also affected by this correction as long as they depend on the evanescent constant

$$\beta_{n,m} = \frac{2}{\Delta z}\sinh^{-1}\Delta z\sqrt{\frac{\sin(kx_n)^2}{\Delta x} + \frac{\sin(ky_m)^2}{\Delta y} - \frac{\sin(kt)^2}{c\Delta t}} \tag{11}$$

where $kt = \omega\Delta t/2$ $kx_n = n\pi\Delta x/2a$, $ky_m = m\pi\Delta y/2b$

$$Z_{\mathrm{TE}_{n,m}} = \frac{\omega\mu}{\beta_{n,m}}. \tag{12}$$

The difference between the results obtained using an analytical and a numerical $\beta_{n,m}$ does not affect the fundamental TE_{10} mode since it is a propagating mode. The numerical dispersion only has a strong influence on the phase constant. The results for higher order modes using analytical $\beta_{n,m}$, differ in 5%–12% from the ones calculated using the numerical dispersive value (8–10-GHz frequency band). The difference increases with the orders of the modes; in our results, the deviation is larger for the $\mathrm{TE}_{3,2}$ mode. Fig. 4 shows how this error depends on the distance from the sampling plane to the reference plane. Fig. 4 is for $S_{1,j}$, $j = 5, 6, 7, 8$ at the central frequency (9 GHz). The FDTD parameters calculated with numerical $\beta_{n,m}$ are plotted in Fig. 5. These results are compared with results without the dispersive correction and results obtained by the mode-matching (MM) technique. The present results were obtained using 3000 FDTD time iterations, which took around 20 min of CPU time in a 486 personal computer.

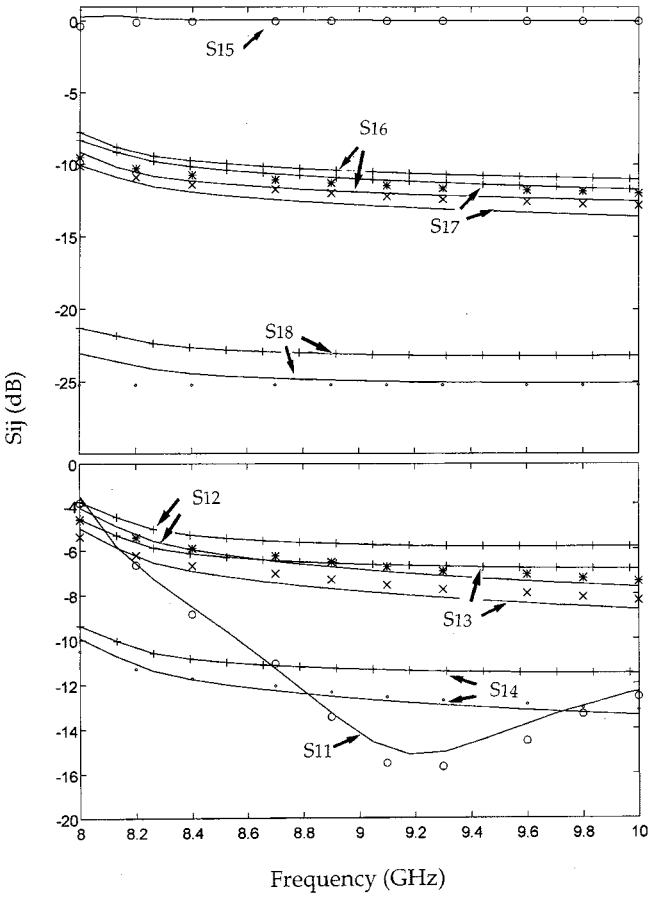

Fig. 5. Multimode transmission and reflection parameters for the discontinuity of Fig. 3, incident is TE_{10} in waveguide a : (o) $S_{1,5}$, and $S_{1,1}$. $(*)S_{1,6}$, and $S_{1,2}$. $(\times)S_{1,7}$, and $S_{1,3}$. $(\cdot)S_{1,8}$, and $S_{1,4}$. (—): MM results. $(-+-)$: FDTD without correction.

V. Conclusion

A numerical dispersion relation is derived for the numerical modeling of evanescent waves in FDTD. In the numerical domain of FDTD, evanescent waves decay slower than in the analytical space time domain. This numerical dispersion is expected to affect the numerical sampling of the propagating and evanescent modes in the vicinity of a waveguide discontinuity because numerical attenuation is lower than analytical attenuation. FDTD is used to obtain multimode transmission and reflection coefficients of a three-dimensional discontinuity. It is necessary to use the numerical FDTD dispersion relation to correct the obtained multimode parameters in order to achieve a reasonable degree of accuracy in the numerical results.

REFERENCES

[1] K. L. Shlager and J. B. Schneider, "A selective survey of the finite-difference time-domain literature," *IEEE Antennas Propagat. Mag.*, vol. 37, no. 4, pp. 39–56, Aug. 1995.

[2] E. A. Navarro, N. T. Sangary, and J. Litva, "Some considerations on the accuracy of the non uniform FDTD method and its application to waveguide analysis when combined with the perfect matched layer technique," *IEEE Trans. Microwave Theory Tech.*, vol. 44, pp. 1115–1124, July 1996.

[3] A. C. Cangellaris, "Numerical stability and numerical dispersion of compact 2-D/FDTD method used for the dispersion analysis of waveguides," *IEEE Microwave Guided Wave Lett.*, vol. 3, pp. 3–5, Jan. 1993.

[4] F. Alimenti *et al.*, "Modal absorption in the FDTD method: A critical review," *J. Numer. Modeling*, vol. 10, no. 4, pp. 245–264, Apr. 1997.

[5] M. Mrozowski, "A hybrid PEE-FDTD algorithm for accelerated time domain analysis of electromagnetic waves in shielded structures," *IEEE Microwave and Guided Wave Lett.*, vol. 4, no. 10, pp. 323–325, 1994.

[6] L. A. Vielva, J. A. Pereda, A. Prieto, and A. Vegas, "FDTD multimode characterization of waveguide devices using absorbing boundary conditions for propagating and evanescent waves," *IEEE Microwave Guided Wave Lett.*, vol. 4, no. 6, pp. 160–162, 1994.

[7] E. A. Navarro, L. Gallart, J. L. Cruz, B. Gimeno, and V. Such, "Accurate absorbing boundary conditions for the FDTD analysis of H-plane waveguide discontinuities," *Proc. Inst. Elect. Eng.*, vol. 141, no. 1, pp. 59–61, Jan. 1994.

[8] F. Alimenti *et al.*, "Efficient analysis of waveguide components by FDTD combined with time domain modal expansion," *IEEE Microwave Guided Wave Lett.*, vol. 4, no. 10, pp. 351–353, 1995.

[9] J. Berenger, "A perfectly matched layer for the absorption of electromagnetic waves," *J. Comput. Phys.*, vol. 114, pp. 185–200, 1994.

[10] D. S. Katz, E. T. Thiele, and A. Taflove, "Validation and extension to three dimensions of the Berenger PML absorbing boundary condition for FD-TD meshes," *IEEE Microwave Guided Wave Lett.*, vol. 4, no. 8, pp. 268–270, 1994.

[11] E. A. Navarro, C. Wu, P. Y. Chung, and J. Litva, "Application of PML superabsorbing boundary condition to non-orthogonal FDTD method," *Electron. Lett.*, vol. 30, no. 20, pp. 1654–1656, 1994.

[12] J. Fang and Z. Wu, "Generalized perfectly matched layers for the absorption of propagating and evanescent waves in losseless and lossy media," *IEEE Trans. Microwave Theory Tech.*, vol. 44, pp. 2216–2222, Dec. 1996.

[13] J. Berenguer, "An effective PML for the absorption of evanescent waves in waveguides," *IEEE Microwave Guided Wave Lett.*, vol. 8, pp. 188–190, May 1998.

[14] G. E. Forsythe and W. R. Wasow, *Finite-Difference Methods for Partial Differential Equations*. New York: Wiley, 1960.

[15] S. G. Mikhlin and K. L. Smolitskiy, *Approximate Methods for Solution of Differential and Integral Equations*. New York: Elsevier, 1967.

[16] A. Taflove, "Advanced numerical modeling of microwave penetration and coupling for complex structures-Final Report," Lawrence Livermore Nat. Lab., Livermore, CA, Final Rep. UCRL-15960, Sept. 1987.

[17] D. M. Pozar, *Microwave Engineering*. Reading, MA: Addison-Wesley, 1990.

Enrique A. Navarro (M'97) was born in Sueca, València, Spain, in 1965. He received the Licenciado and the Ph.D. degrees from the Universitat de València, València, Spain, in 1988 and 1992, respectively, both in physics.

From 1988 to 1989, he was with the Grupo de Mecánica del Vuelo S.A. (GMV S.A.), Madrid, Spain. Since 1989, he has been teaching and performing research with the Department of Applied Physics, Universitat de València, where he was a Fellow from 1989 to 1991, Assistant Professor from 1991 to 1997, and Professor from 1997. In 1994, he was with the Communications Research Laboratory, McMaster University, Hamilton, Ont., Canada. His current research interests include numerical methods in electromagnetics, microwave passive devices, and intelligent antennas.

Dr. Navarro was the recipient of a 1993 NATO Fellowship.

Thamar M. Bordallo was born in Caudete, Castilla-la Mancha, Spain, on February 15, 1968. She received the Licenciado degree in physics and the Licenciado con Grado degree from the Universitat de València, València, Spain, in 1992 and 1995, respectively, and is currently working toward the Ph.D. degree in the field of numerical techniques for analyzing microwave passive devices at the Universitat de València.

Since 1992, she has been with the Department of Applied Physics, Universitat de València, where she is involved with electromagnetic beams, numerical techniques, and near-field measurements. She is a Secondary School Teacher at the Martin Sorolla School, València, Spain.

Joaquín Navasquillo-Miralles was born in Carlet, València, Spain, on April 21, 1978. He graduated (honors) from the Eduardo Primo High School, Carlet, Spain, and is currently working toward the M.S. degree in communications at the Universitat Politécnica de València, València, Spain.

Since 1996, he has been collaborating with the Electromagnetics Group, Department of Applied Physics, Universitat de València. His current research interests include numerical techniques in electromagnetics and microwave measurements.